Joint Iterative Time-Variant Channel Estimation and Multi-User Detection for MIMO-OFDM Systems

Pierluigi SALVO ROSSI and Ralf R. MÜLLER
Department of Electronics and Telecommunications, Norwegian University of Science and Technology
O.S. Bragstads plass 2B, 7491 Trondheim, Norway, Email: {salvoros,mueller}@iet.ntnu.no

***Abstract*—This paper presents an iterative receiver for Multiple-Input Multiple-Output (MIMO) Orthogonal Frequency Division Multiplexing (OFDM) systems. The receiver performs channel estimation and multi-user detection, with soft information iteratively provided by the single-user decoders. Time-variance is effectively taken into account exploiting the properties of the discrete prolate spheroidal (DPS) sequences. Simulation results for the performance are presented in terms of Bit Error Rate (BER) vs Signal-to-Noise Ratio (SNR), showing how the Single-User Bound (SUB) is approached in a few iterations.**

I. INTRODUCTION

Wireless communications play a central role in the modern society of information. The increasing demand of multimedia services, mobility requirements up to vehicular speed, the intrinsic problems affecting the radio channel, pose significant challenges in designing high-data-rate communication systems. Wireless broadband communications for mobile users with quality of service comparable to wireline technologies are among the most critical tasks.

Use of multiple antennas at both transmit and receiver side, providing a Multiple-Input Multiple-Output (MIMO) channel, is a very popular solution to obtain either a diversity gain or a capacity gain [8], [22]. As for the latter, MIMO systems are capable of increasing capacity by a factor of the minimum number of transmit and receive antennas, thus appearing very suited to future services. Orthogonal Frequency Division Multiplexing (OFDM) is a technique for high-data-rate transmissions adopted in several standards [8], [22]. OFDM converts a frequency-selective channel into a set of frequency-flat subchannels, thus requiring lower complexity for channel equalization compared to single-carrier transmissions. The separation between adjacent subchannels is the minimum required to preserve orthogonality, in order to have high spectral efficiency. OFDM for MIMO channels have been studied to mitigate inter-symbol interference and enhance system capacity at the same time [10], [21]. MIMO-OFDM systems appear to be the natural choice for wireless high-data-rate communications.

Iterative (turbo) receivers achieve excellent performance with contained complexity, thus representing a very attractive technique for next generation systems [2], [6], [7], [19], [24]. Like in standard Multi-User Detection (MUD) [23], Multiple Access Interference (MAI) is not treated as noise. MUD and single-user decoding are decoupled into separate problems, iteratively exchanging each other their results via soft information. Iterative receivers have shown to be attractive also for MIMO-OFDM systems [9], [11], [13], although channel estimation has not benefited of the iterative structure. It has been shown, in different scenarios, that the iterative structure of the receiver can also include channel estimation and still be very well performing [12], [26]. When mobility is a critical issue to be addressed, time-variation of the channel is efficiently and accurately taken into account by exploiting the properties of the discrete prolate spheroidal (DPS) sequences [20], [25]. A very recent work [1] takes into account joint channel estimation and MUD in MIMO-OFDM systems combined with the use of turbo-codes [5], [14].

This paper proposes an iterative receiver for MIMO-OFDM systems performing joint time-variant channel estimation and MUD, with the use of convolutional codes [14], [15]. It is organized as follows: the mathematical model for the considered MIMO-OFDM system is described in Section II; in Section III we develop the structure of the iterative receiver; Section IV shows and compares the performance obtained via numerical simulations; some concluding remarks are given in Section V.

Notation - Column vectors (resp. matrices) are denoted with lower-case (resp. upper-case) bold letters; a_i (resp. $A_{i,j}$) denotes the ith (resp. (i,j)th) element of vector $\boldsymbol{a}$ (resp. matrix $\boldsymbol{A}$); $\mathrm{diag}(\boldsymbol{a})$ denotes a diagonal matrix whose main diagonal is $\boldsymbol{a}$. $\boldsymbol{I}_N$ denotes the $N \times N$ identity matrix; $\boldsymbol{i}_N^{(n)}$ denotes the nth column of $\boldsymbol{I}_N$; $\boldsymbol{e}_N$ (resp. $\boldsymbol{o}_N$) denotes a vector of length N whose elements are 1 (resp. 0); $\mathbb{E}\{.\}$, $(.)^*$, $(.)^{\mathrm{T}}$ and $(.)^{\mathrm{H}}$ denote expectation, conjugate, transpose and conjugate transpose operators; $\delta_{n,m}$ denotes the Kronecker delta; $\otimes$ denotes the Kronecker matrix product; $\lceil a \rceil$ denotes the smallest integer value greater or equal than a; $\jmath$ denotes the imaginary unit; the symbol $\sim$ means "distributed as".

II. SYSTEM MODEL

We consider a MIMO-OFDM system with K transmit antennas, N receive antennas, M subcarriers. We also assume that each transmit antenna sends an independent data stream and we consider equivalent the terms "user" and "transmit antenna"[1]. The model for the transmitter at the generic transmit

[0]This work has been supported by the Research Council of Norway under WILATI project within the NORDITE framework.

[1]The model can be referred to the case in which K users are provided with one single transmit antenna as well as to the case in which one single user is provided with K transmit antennas and its data stream is parallelized in K independent data streams.

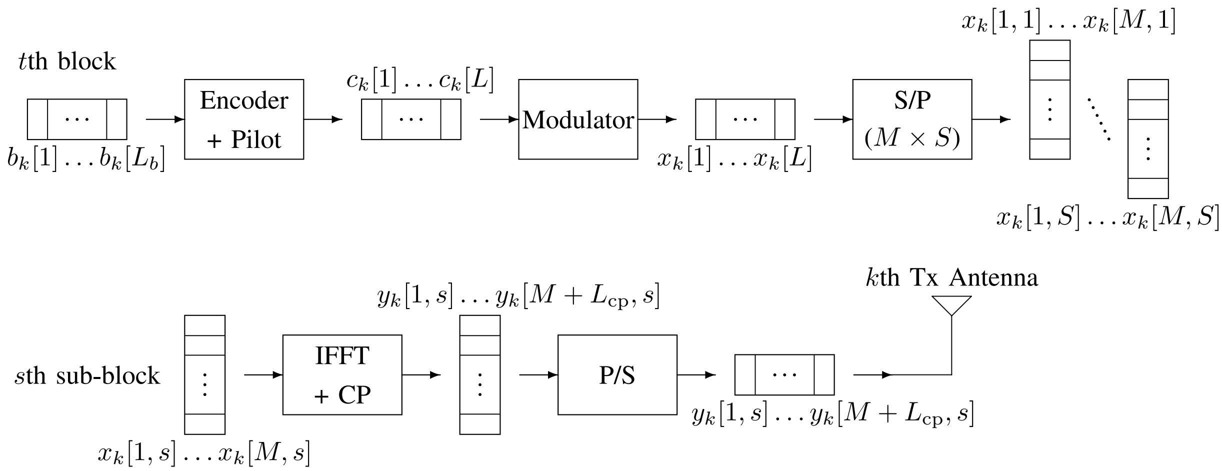

Fig. 1. Block diagram for the transmitter.

antenna is shown in Fig. 1. The transmission is frame oriented: the bit stream is divided in blocks of L_b source bits; each block is encoded via a convolutional encoder and a random interleaver [14], [15]; L_p pilot bits are inserted to produce a frame of L code bits. The bits of the frame are mapped into symbols via Binary Phase Shift Keying (BPSK) modulation [15], thus in the following we use the term frame to denote both the bits or the BPSK symbols. The frame is divided into $S = L/M$ blocks, and each block gives rise to an OFDM symbol to be transmitted on the wireless channel.

We assume that both L and L_p are integer multiples of M, thus we have $S_p = L_p/M$ pilot OFDM symbols and $S - S_p$ data OFDM symbols. Optimal pilot placement falls beyond the scope of this paper, and we simply assume that pilot OFDM symbols are distributed in the frame according to the set of indexes $\left\{ \left\lceil \frac{(2s-1)S}{2S_p} \right\rceil \right\}_{s=1}^{S_p}$.

In the following: $b_k[\ell]$ and $c_k[\ell]$ respectively denote the ℓth source bit and the ℓth code bit (including pilots) to be transmitted by the kth transmit antenna; $x_k[m,s]$ denotes the (*Frequency Domain*) symbol transmitted by the kth transmit antenna on the mth subcarrier during transmission of the sth OFDM symbol ($y_k[m,s]$ corresponds in *Time Domain*); $H_{n,k}[m,s]$ denotes the (*Frequency Domain*) channel coefficient between the kth transmit antenna and the nth receive antenna on the mth subcarrier during transmission of the sth OFDM symbol; $w_n[m,s]$ denotes the (*Frequency Domain*) additive noise at the nth receive antenna on the mth subcarrier during transmission of the sth OFDM symbol; $r_n[m,s]$ denotes the (*Frequency Domain*) received signal at the nth receive antenna on the mth subcarrier during transmission of the sth OFDM symbol ($q_n[m,s]$ corresponds in *Time Domain*).

We denote the transmitted vector, the channel matrix, the noise vector ($\sim \mathcal{CN}(\mathbf{0}, \sigma_w^2 \boldsymbol{I}_N)$), and the received vector as

$$\begin{aligned}
\boldsymbol{x}[m,s] &= (x_1[m,s],\dots,x_K[m,s])^{\mathrm{T}} \\
\boldsymbol{H}[m,s] &= \begin{pmatrix} H_{1,1}[m,s] & \dots & H_{1,K}[m,s] \\ \vdots & \ddots & \vdots \\ H_{N,1}[m,s] & \dots & H_{N,K}[m,s] \end{pmatrix}, \\
\boldsymbol{w}[m,s] &= (w_1[m,s],\dots,w_N[m,s])^{\mathrm{T}}, \\
\boldsymbol{r}[m,s] &= (r_1[m,s],\dots,r_N[m,s])^{\mathrm{T}},
\end{aligned}$$

and assume that the length of the cyclic prefix (L_{cp}) exceeds the channel delay spread, then the discrete-time model for the received signal is

$$\boldsymbol{r}[m,s] = \boldsymbol{H}[m,s]\boldsymbol{x}[m,s] + \boldsymbol{w}[m,s]\,. \tag{1}$$

Also we denote the channel vector from kth transmit antenna as $\boldsymbol{h}_{(k)}[m,s] = \boldsymbol{H}[m,s]\boldsymbol{i}_K^{(k)}$.

It is worth noticing that m and s represent frequency-variation and time-variation, respectively.

III. Iterative Receiver

Transmissions from the various antennas combine at each receive antenna and are processed according to the receiver model shown in Fig. 2. OFDM robustness to synchronization errors allows to ignore time asynchrony among transmit antennas (assuming that synchronization errors do not exceed the length of the cyclic prefix). Each OFDM symbol is demodulated and sent to the iterative decoder, which performs three fundamental tasks:

- *MUD* - processing received data from the demodulator, code extrinsic information from the Soft-Input Soft-Output (SISO) decoders, and channel estimates from the channel estimator; furnishing symbol extrinsic information to the SISO decoders. This task is realized via

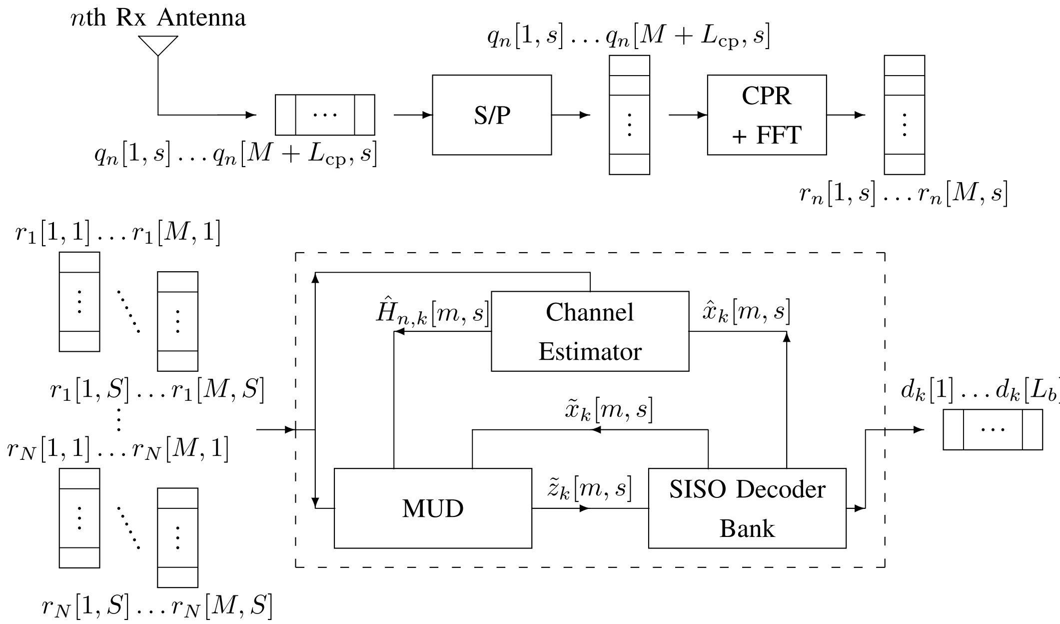

Fig. 2. Block diagram for the receiver.

Parallel Interference Cancellation (PIC) and Minimum Mean Square Error (MMSE) filtering [12], [24], [26].

- *SISO Decoding* - processing symbol extrinsic information from the MUD; furnishing code extrinsic information to the MUD, code *a posteriori* information to the channel estimator, source *a posteriori* information as final output. This task is realized via Bahl-Cocke-Jelinek-Raviv (BCJR) algorithm [3], [4], [14].
- *Channel Estimation* - processing received data from the demodulator and code *a posteriori* information from the SISO decoders; furnishing channel estimates to the MUD. This task is realized via Slepian Basis Expansion (SBE) and Linear MMSE (LMMSE) estimation [25], [26].

Both MUD and SISO decoders exchange extrinsic-based soft information on symbols x_k. We denote $\tilde{x_k}$ the one passing from the SISO decoders to the MUD, and $\tilde{z_k}$ the one passing from the MUD to the SISO decoders. SISO decoders also provide *a posteriori*-based soft information on symbol x_k, denoted $\hat{x_k}$, to the channel estimator, and *a posteriori*-based soft information on source bit, denoted d_k. The channel estimator provides channel coefficient estimates, denoted $\hat{H}_{n,k}$.

It is worth noticing that $\{\tilde{z_k}[1],\dots,\tilde{z_k}[L]\}$ are deinterleaved before being passed to the the SISO decoder, while $\{\tilde{x_k}[1],\dots,\tilde{x_k}[L]\}$ and $\{\hat{x_k}[1],\dots,\hat{x_k}[L]\}$ are interleaved before being passed to the MUD and to the channel estimator, respectively. In the following, to simplify notation, we do NOT introduce different notations in order to explicitly distinguish interleaved and deinterleaved symbols, and leave the meaning to be evinced from the context.

A. MUD

As previously said, MUD is performed via PIC and MMSE filtering. More precisely, the received signals (1) are processed separately for each subcarrier and for each OFDM symbol. We omit the indexes m and s to simplify notation. Also, in the derivation of the symbol extrinsic soft information, we assume that the receiver has perfect knowledge of the channel coefficients, while in practice estimates from the channel estimator are used ($\boldsymbol{H}$ is replaced with $\hat{\boldsymbol{H}}$).

The PIC block receives $\tilde{\boldsymbol{x}}$ from the SISO decoders and $\boldsymbol{H}$ from the channel estimators. The interference component for the kth transmit antenna is $\boldsymbol{H}\tilde{\boldsymbol{x}}_{(k)}$, where $\tilde{\boldsymbol{x}}_{(k)} = \tilde{\boldsymbol{x}} - \tilde{x}_k \boldsymbol{i}_K^{(k)}$, then for each transmit antenna it is possible to compute the residual term from the interference cancellation as

$$\tilde{\boldsymbol{r}}_{(k)} = \boldsymbol{r} - \boldsymbol{H}\tilde{\boldsymbol{x}}_{(k)} \ . \tag{2}$$

The residual term is then processed with an MMSE filter, in order to reduce further the effects of noise and MAI, giving the extrinsic-based soft information

$$\tilde{z}_k = \boldsymbol{f}_{(k)}^{\mathrm{H}} \tilde{\boldsymbol{r}}_{(k)} \ .$$

The filter is found as $\boldsymbol{f}_{(k)} = \arg\min_{\boldsymbol{f}} \mathbb{E}\left\{|x_k - \boldsymbol{f}^{\mathrm{H}}\tilde{\boldsymbol{r}}_{(k)}|^2\right\}$ $= \left(\mathbb{E}\left\{\tilde{\boldsymbol{r}}_{(k)}\tilde{\boldsymbol{r}}_{(k)}^{\mathrm{H}}\right\}\right)^{-1} \mathbb{E}\left\{x_k \tilde{\boldsymbol{r}}_{(k)}\right\}$. From (1) and (2) we have

$$\begin{aligned} \mathbb{E}\left\{\tilde{\boldsymbol{r}}_{(k)}\tilde{\boldsymbol{r}}_{(k)}^{\mathrm{H}}\right\} &= \boldsymbol{H}\boldsymbol{V}_{(k)}\boldsymbol{H}^{\mathrm{H}} + \sigma_w^2 \boldsymbol{I}_N \ , \\ \mathbb{E}\left\{x_k \tilde{\boldsymbol{r}}_{(k)}\right\} &= \boldsymbol{h}_{(k)} \ , \end{aligned}$$

being $\boldsymbol{V}_{(k)} = \mathrm{diag}\left((1-|\tilde{x}_1|^2, \dots, 1-|\tilde{x}_{k-1}|^2, 1, 1-|\tilde{x}_{k+1}|^2, \dots, 1-|\tilde{x}_K|^2)\right)$, thus giving

$$\tilde{z}_k = \boldsymbol{h}_{(k)}^{\mathrm{H}} \left(\boldsymbol{H}\boldsymbol{V}_{(k)}\boldsymbol{H}^{\mathrm{H}} + \sigma_w^2 \boldsymbol{I}_N\right)^{-1} \tilde{\boldsymbol{r}}_{(k)} \ .$$

The unbiased estimate is then

$$\begin{aligned} \tilde{z}_k &= \frac{\boldsymbol{h}_{(k)}^{\mathrm{H}} \left(\boldsymbol{H}\boldsymbol{V}_{(k)}\boldsymbol{H}^{\mathrm{H}} + \sigma_w^2 \boldsymbol{I}_N\right)^{-1} \tilde{\boldsymbol{r}}_{(k)}}{\boldsymbol{h}_{(k)}^{\mathrm{H}} \left(\boldsymbol{H}\boldsymbol{V}_{(k)}\boldsymbol{H}^{\mathrm{H}} + \sigma_w^2 \boldsymbol{I}_N\right)^{-1} \boldsymbol{h}_{(k)}} \\ &= \frac{\boldsymbol{i}_K^{(k)\mathrm{T}} \left(\boldsymbol{H}^{\mathrm{H}}\boldsymbol{H} + \sigma_w^2 (\boldsymbol{V}_{(k)})^{-1}\right)^{-1} \boldsymbol{H}^{\mathrm{H}} \tilde{\boldsymbol{r}}_{(k)}}{\boldsymbol{i}_K^{(k)\mathrm{T}} \left(\boldsymbol{H}^{\mathrm{H}}\boldsymbol{H} + \sigma_w^2 (\boldsymbol{V}_{(k)})^{-1}\right)^{-1} \boldsymbol{H}^{\mathrm{H}} \boldsymbol{h}_{(k)}} \ , \end{aligned} \quad (3)$$

where the last identity is obtained using the matrix inversion lemma. It is worth noticing that (3) is the output of a "conditional" filter, as it is obtained on the basis of the soft estimates for each single symbol, for each iteration, for each subcarrier, for each OFDM symbol.

B. SISO Decoders

After collecting $\{z_k[1], \dots, z_k[L]\}$, each transmit antenna can be decoded independently using the BCJR algorithm [3], [4], [14]. It is worth noticing that $z_k[\ell]$ has been transmitted on the mth subcarrier during the sth OFDM symbol if $\ell = (s-1)M + m$. The model for the output of the MUD [24], used by the single SISO decoder for the kth transmit antenna, is $z_k = \mu_k x_k + v_k$, with $v_k \sim \mathcal{CN}(0, \eta_k^2)$, where $\mu_k = 1$, and

$$\eta_k^2 = \frac{1}{\boldsymbol{i}_K^{(k)\mathrm{T}} \left(\boldsymbol{H}^{\mathrm{H}}\boldsymbol{H} + \sigma_w^2 \boldsymbol{I}_N\right)^{-1} \boldsymbol{H}^{\mathrm{H}} \boldsymbol{h}_{(k)}} \ .$$

We omit the index k to simplify notation.

We use a trellis representation for the code, and denote $\varsigma_t \in \{1, \dots, Q\}$ the state of the trellis at the end of the tth transition among T total transitions. The tth transition corresponds to the tth group of source bits entering the encoder [14], [15]. Forward and backward variables are computed according to the following recursions:

$$\alpha_t(j) = \sum_{i=1}^{Q} \alpha_{t-1}(i)\gamma_t(i,j) \ , \ \beta_t(i) = \sum_{j=1}^{Q} \gamma_{t+1}(i,j)\beta_{t+1}(j) \ ,$$

where the initialization is given by $\alpha_0(i) = \delta_{i,1}$ and $\beta_T(j) = \delta_{j,1}$, and where $\gamma_t(i,j) = \Pr(\varsigma_t = j | \varsigma_{t-1} = i) \times \prod_{o=1}^{n_0} \Pr\left(z[(t-1)n_0 + o] | x_{i\to j}[(t-1)n_0 + o]\right)$, being $x_{i\to j}[(t-1)n_0 + o]$ the oth symbol among the n_0 that would have been transmitted during the tth transition with $\varsigma_{t-1} = i$ and $\varsigma_t = j$. The initialization of the forward and backward variables takes into account the fact that the encoder starts in state 1 and, due to the insertion of appropriate tail bits to the block of source bits within the frame, also stops in state 1.

The *a posteriori* likelihood and the extrinsic likelihood are obtained respectively as

$$\Lambda_{\mathrm{APP}}(x[\ell] | z[1], \dots, z[L]) = \frac{\sum_{(i,j):x[\ell]=+1} \alpha_{t-1}(i)\gamma_t(i,j)\beta_t(j)}{\sum_{(i,j):x[\ell]=-1} \alpha_{t-1}(i)\gamma_t(i,j)\beta_t(j)} \ ,$$

$$\Lambda_{\mathrm{EXT}}(x[\ell] | z[1], \dots, z[L]) = \frac{\Lambda_{\mathrm{APP}}(x[\ell] | z[1], \dots, z[L])}{\frac{\Pr(z[\ell]|x[\ell]=+1)}{\Pr(z[\ell]|x[\ell]=-1)}} \ ,$$

being [3], [14] $\Pr(z|x) = \frac{1}{\sqrt{2\pi\eta^2}} \exp\left(-\frac{|z-\mu x|^2}{2\eta^2}\right)$.

More specifically, the algorithm is implemented in the log-domain [17], exploiting the Jacobian logarithm $\log\left(\mathrm{e}^{\delta_1} + \mathrm{e}^{\delta_2}\right) = \max(\delta_1, \delta_2) + \log\left(1 + \mathrm{e}^{-|\delta_2 - \delta_1|}\right)$.

C. Channel Estimation

We consider a channel with normalized Doppler bandwidth $\nu_{\max}^{(\mathrm{D})}$ and Doppler Spectrum for the mth subcarrier between the kth transmit antenna and the nth receive antenna

$$H_{n,k}^{(\mathrm{D})}(m,\nu) = \sum_{s=-\infty}^{+\infty} H_{n,k}(m,s) \exp(-\jmath 2\pi\nu s) \ .$$

We make use of the SBE [25], [26]

$$\hat{H}_{n,k}(m,s) \approx \sum_{i=1}^{I} \psi_{n,k}[m,i] u_i[s] \ , \quad (4)$$

where $u_i[s]$ is the sth sample of the ith DPS sequence [20] defined as the solution to

$$\sum_{s'=1}^{S} 2\nu_{\max}^{(\mathrm{D})} \mathrm{sinc}\left(2\nu_{\max}^{(\mathrm{D})}(s'-s)\right) u_i[s'] = \lambda_i(\nu_{\max}^{(\mathrm{D})}, S) u_i[s] \ ,$$

and $S_{\mathrm{D}} \le I \le S$, being $S_{\mathrm{D}} = \left\lceil 2\nu_{\max}^{(\mathrm{D})} S \right\rceil + 1$ the approximate signal space dimension. The reason behind the reduction of the space dimension is that the eigenvalues $\lambda_i(\nu_{\max}^{(\mathrm{D})}, S)$ rapidly become negligible for $i > 2\nu_{\max}^{(\mathrm{D})} S$.

The SBE makes use of an orthogonal basis based on DPS sequences, that have shown to be the bandlimited sequences simultaneously most concentrated in a finite time interval [20]. Advantage of using the SBE is twofold: (i) low complexity, the reduction of the space dimension means less coefficients to be estimated; (ii) high accuracy, no assumption on the stochastic model for the channel is needed but only knowledge of the maximum Doppler spread.

From (1) and (4), denoting

$$\begin{aligned} \boldsymbol{u}[s] &= (u_1[s], \dots, u_I[s])^{\mathrm{T}} \ , \\ \boldsymbol{\xi}[m,s] &= \boldsymbol{x}[m,s] \otimes \boldsymbol{u}[s] \ , \\ \boldsymbol{\Xi}[m,s] &= \boldsymbol{I}_N \otimes \boldsymbol{\xi}[m,s]^{\mathrm{T}} \ , \\ \boldsymbol{\psi}_{n,k}[m] &= (\psi_{n,k}[m,1], \dots, \psi_{n,k}[m,I])^{\mathrm{T}} \ , \\ \boldsymbol{\psi}_n[m] &= \left(\boldsymbol{\psi}_{n,1}[m]^{\mathrm{T}}, \dots, \boldsymbol{\psi}_{n,K}[m]^{\mathrm{T}}\right)^{\mathrm{T}} \ , \\ \boldsymbol{\psi}[m] &= \left(\boldsymbol{\psi}_1[m]^{\mathrm{T}}, \dots, \boldsymbol{\psi}_N[m]^{\mathrm{T}}\right)^{\mathrm{T}} \ , \end{aligned}$$

we get $\boldsymbol{r}[m,s] = \boldsymbol{\Xi}[m,s]\boldsymbol{\psi}[m] + \boldsymbol{w}[m,s]$, and finally, collecting all the OFDM received symbols and denoting

$$\begin{aligned} \boldsymbol{r}[m] &= \left(\boldsymbol{r}[m,1]^{\mathrm{T}}, \dots, \boldsymbol{r}[m,S]^{\mathrm{T}}\right)^{\mathrm{T}} \ , \\ \boldsymbol{\Xi}[m] &= \left(\boldsymbol{\Xi}[m,1]^{\mathrm{T}}, \dots, \boldsymbol{\Xi}[m,S]^{\mathrm{T}}\right)^{\mathrm{T}} \ , \\ \boldsymbol{w}[m] &= \left(\boldsymbol{w}[m,1]^{\mathrm{T}}, \dots, \boldsymbol{w}[m,S]^{\mathrm{T}}\right)^{\mathrm{T}} \ , \end{aligned}$$

we obtain the signal model for the channel estimation as

$$\boldsymbol{r}[m] = \boldsymbol{\Xi}[m]\boldsymbol{\psi}[m] + \boldsymbol{w}[m] \ . \quad (5)$$

1930-529X/07/$25.00 © 2007 IEEE
This full text paper was peer reviewed at the direction of IEEE Communications Society subject matter experts for publication in the IEEE GLOBECOM 2007 proceedings.

We omit the index m to simplify notation. We restrict our attention to linear channel estimators, i.e. $\hat{\boldsymbol{\psi}} = \boldsymbol{A}_{\psi}\boldsymbol{r}$, where is given by $\boldsymbol{A}_{\psi} = \arg\min_{\boldsymbol{A}} \mathbb{E}\left\{|\boldsymbol{\psi} - \boldsymbol{A}\boldsymbol{r}|^2\right\} = \left(\left(\mathbb{E}\left\{\boldsymbol{r}\boldsymbol{r}^{\mathrm{H}}\right\}\right)^{-1}\mathbb{E}\left\{\boldsymbol{r}\boldsymbol{\psi}^{\mathrm{H}}\right\}\right)^{\mathrm{H}}$. From (5) we have $\mathbb{E}\left\{\boldsymbol{r}\boldsymbol{r}^{\mathrm{H}}\right\} = \mathbb{E}\left\{\boldsymbol{\Xi}\boldsymbol{C}_{\psi}\boldsymbol{\Xi}^{\mathrm{H}}\right\} + \sigma_w^2\boldsymbol{I}_{SN}$ and $\mathbb{E}\left\{\boldsymbol{r}\boldsymbol{\psi}^{\mathrm{H}}\right\} = \hat{\boldsymbol{\Xi}}\boldsymbol{C}_{\psi}$, being $\boldsymbol{C}_{\psi} = \mathbb{E}\left\{\boldsymbol{\psi}\boldsymbol{\psi}^{\mathrm{H}}\right\} = \frac{1}{2\nu_{\max}^{(\mathrm{D})}}\mathrm{diag}\left(\boldsymbol{\lambda}_{\psi}\right)$, $\boldsymbol{\lambda}_{\psi} = \boldsymbol{e}_{NK} \otimes \boldsymbol{\lambda}$, $\boldsymbol{\lambda} = (\lambda_1, \ldots, \lambda_I)^{\mathrm{T}}$, and $\hat{\boldsymbol{\Xi}} = \mathbb{E}\{\boldsymbol{\Xi}\}$. The diagonal structure of $\boldsymbol{C}_{\psi}$ is due to the independence of channels among different transmit antennas and/or receive antennas, and to the orthogonality of the DPS sequences, i.e.

$$\mathbb{E}\left\{\psi_{n',k'}[m,i]\psi^*_{n'',k''}[m,j]\right\} = \frac{\lambda_i}{2\nu_{\max}^{(\mathrm{D})}}\delta_{n',n''}\delta_{k',k''}\delta_{i,j} \ .$$

The independence of transmit antennas and also of OFDM symbols (due to the effect of random interleaving), i.e

$$\mathbb{E}\left\{x_{k'}[m,s']x^*_{k''}[m,s'']\right\} = \begin{cases} 1 & k'=k'', s'=s'' \\ \hat{x}_{k'}[m,s']\hat{x}^*_{k''}[m,s''] & \text{else} \end{cases} ,$$

gives

$$\mathbb{E}\left\{\boldsymbol{\Xi}\boldsymbol{C}_{\psi}\boldsymbol{\Xi}^{\mathrm{H}}\right\} = \begin{pmatrix} \boldsymbol{\Phi}_{1,1} & \cdots & \boldsymbol{\Phi}_{1,S} \\ \vdots & \ddots & \vdots \\ \boldsymbol{\Phi}_{S,1} & \cdots & \boldsymbol{\Phi}_{S,S} \end{pmatrix} ,$$

being $\boldsymbol{\Phi}_{s,s'} = \mathrm{diag}(\phi_{s,s'}\boldsymbol{e}_N)$ with

$$\phi_{s,s'} = \begin{cases} \sum_{i=1}^{I}\sum_{k=1}^{K} \frac{\lambda_i}{2\nu_{\max}^{(\mathrm{D})}}|u_i[s]|^2 & s = s' \\ \sum_{i=1}^{I}\sum_{k=1}^{K} \frac{\lambda_i}{2\nu_{\max}^{(\mathrm{D})}}u_i[s]u_i^*[s']\hat{x}_k[m,s]\hat{x}_k^*[m,s'] & \text{else} \end{cases}$$

It is straightforward to obtain $\mathbb{E}\left\{\boldsymbol{\Xi}\boldsymbol{C}_{\psi}\boldsymbol{\Xi}^{\mathrm{H}}\right\} = \hat{\boldsymbol{\Xi}}\boldsymbol{C}_{\psi}\hat{\boldsymbol{\Xi}}^{\mathrm{H}} + \boldsymbol{\Theta}$, being $\boldsymbol{\Theta} = \mathrm{diag}(\boldsymbol{\vartheta} \otimes \boldsymbol{e}_N)$, $\boldsymbol{\vartheta} = (\vartheta_1, \ldots, \vartheta_S)^{\mathrm{T}}$, and $\vartheta_s = \sum_{i=1}^{I}\sum_{k=1}^{K}\frac{\lambda_i}{2\nu_{\max}^{(\mathrm{D})}}|u_i[s]|^2\left(1 - |\hat{x}_k[m,s]|^2\right)$, and finally

$$\boldsymbol{A}_{\psi}^{\mathrm{H}} = \left(\hat{\boldsymbol{\Xi}}\boldsymbol{C}_{\psi}\hat{\boldsymbol{\Xi}}^{\mathrm{H}} + \boldsymbol{\Delta}\right)^{-1}\hat{\boldsymbol{\Xi}}\boldsymbol{C}_{\psi} \ ,$$

with $\boldsymbol{\Delta} = \boldsymbol{\Theta} + \sigma_w^2\boldsymbol{I}_{SN}$.

The channel estimate is obtained as

$$\begin{aligned} \hat{\boldsymbol{\psi}} &= \boldsymbol{C}_{\psi}\hat{\boldsymbol{\Xi}}^{\mathrm{H}}\left(\hat{\boldsymbol{\Xi}}\boldsymbol{C}_{\psi}\hat{\boldsymbol{\Xi}}^{\mathrm{H}} + \boldsymbol{\Delta}\right)^{-1}\boldsymbol{r} \ , \\ &= \left(\hat{\boldsymbol{\Xi}}^{\mathrm{H}}\boldsymbol{\Delta}^{-1}\hat{\boldsymbol{\Xi}} + \boldsymbol{C}_{\psi}^{-1}\right)^{-1}\hat{\boldsymbol{\Xi}}^{\mathrm{H}}\boldsymbol{\Delta}^{-1}\boldsymbol{r} \ , \end{aligned}$$

to be used in (4). The last equality, obtained using the matrix inversion lemma, replaces the inversion of a $SN \times SN$ matrix with the inversion of a $NKI \times NKI$ matrix, saving computations when $K < 1/(2\nu_{\max}^{(\mathrm{D})})$. Also it is worth noticing that both $\boldsymbol{C}_{\psi}$ and $\boldsymbol{\Delta}$ are diagonal, thus their inversion is not computationally prohibitive.

IV. Simulation Results

Numerical performance in terms of Bit Error Rate (BER) vs Signal-to-Noise Ratio (SNR) have been obtained for various systems, and compared with the Single-User Bound (SUB) performance. SUB, used as a reference, represents the performance achieved by a system with a single transmit antenna and perfect knowledge of channel coefficients at the receiver.

Results shown here refer to systems with $M = 32$ subcarriers and $S = 128$ OFDM symbols per frame thus corresponding to $L = 4,096$ code bits per frame. In each frame we used $S_p = 12$ pilot OFDM symbols (less than 10%). Excluding pilots we have $3,712$ code bits generated at rate $R = 1/2$ via a recursive systematic convolutional encoder [15] with generators $(7,5)_8$ and with two tail bits used to enforce the final state into 1, thus $L_b = 1,854$ source bits per frame.

Also, results have been obtained for synthetic-generated channel coefficients. Time-variant channels have been simulated using a Rayleigh fading model according to Jakes'model [16], [25], [27]. Channel coefficients for each transmit-receive antenna pair and for each subcarrier have been generated according to a model with 15 interfering paths and maximum normalized Doppler frequency $\nu_{\max}^{(\mathrm{D})} = 0.005$. The signal space dimension is reduced from $S = 128$ to $S_{\mathrm{D}} = 2$, and we used $I = 5$ coefficients for each SBE.

Fig. 3 refers to a system with $N = 2$ receive antennas and $K = 2$ transmit antennas (2×2 system), while Fig. 4 refers to a system with $N = 4$ receive antennas and $K = 4$ transmit antennas (4×4 system). They show how after a few iterations the receiver approaches the SUB performance. Methods in [9], [10] have shown to perform respectively 1 dB and 1.6 dB away (or worse) from performance with perfect channel knowledge at the receiver. Simulations showed how the receiver we have proposed in this paper, performing joint iterative channel estimation and decoding, approaches the SUB performance with vanishing degradation for reasonable SNRs.

Other recent works [1], [13] focus on using more sophisticated codes as turbo-codes and low-density parity check codes. To give an idea of the proposed framework we compare the performance with those reported in [1]. We notice that in order to achieve a BER$= 10^{-2}$ our system presents a reduction of the required SNR of 1.5 dB in the case of a 2×2 system, and 4.75 dB in the case of a 4×4 system. On the contrary, the system in [1] achieves arbitrary small performance at SNR$= 8.75$ dB in the case of a 2×2 system, and at SNR$= 7.75$ dB in the case of a 4×4 system, due to the waterfall effect of turbo-codes [5], [14], while our systems at the corresponding SNRs only achieve BER$= 3 \cdot 10^{-4}$ and BER$= 2 \cdot 10^{-7}$, respectively. Also it is worth noticing that performance in [1] refers to a number of subcarriers $M = 128$, a channel with 7 paths, a normalized Doppler bandwidth $\nu_{\max}^{(\mathrm{D})} = 0.003$ and use of Quadrature Phase Shift Keying modulation [15].

We are currently working to include use of turbo-codes in our framework. In this case both the global receiver and the single-user decoder present an iterative structure, thus analyzing the impact of the scheduling is crucial for better trade-off performance and complexity. Also, we are testing the proposed system on real MIMO channels [18] with measurements provided by *Lund University* and *Helsinki University of Technology*.

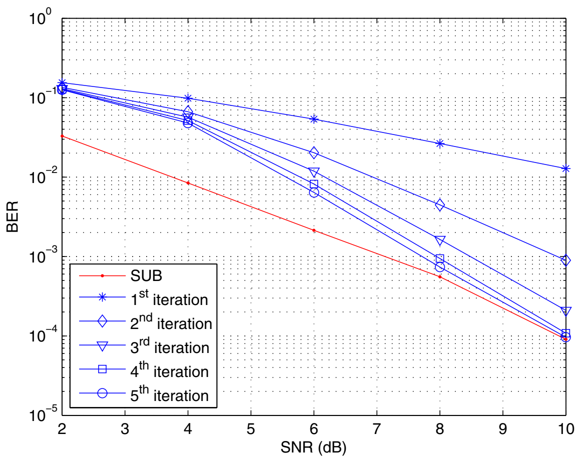

Fig. 3. BER-vs-SNR. Simulation results for a system with $N = 2$, $K = 2$, $M = 32$, $S = 128$, $S_p = 12$, $\nu_{\max}^{(\mathrm{D})} = 0.005$.

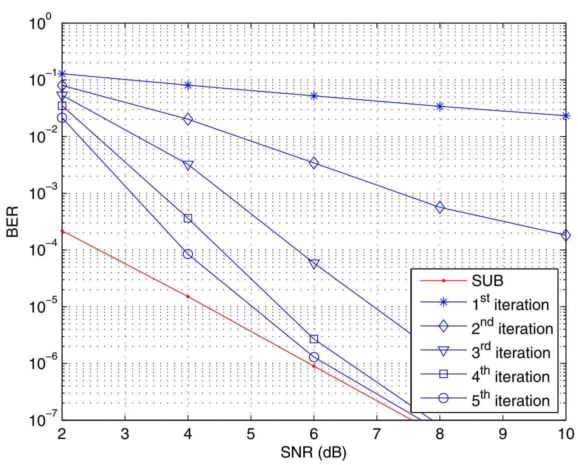

Fig. 4. BER-vs-SNR. Simulation results for a system with $N = 4$, $K = 4$, $M = 32$, $S = 128$, $S_p = 12$, $\nu_{\max}^{(\mathrm{D})} = 0.005$.

V. Conclusion

An iterative receiver for joint time-variant channel estimation and multi-user detection in MIMO-OFDM systems has been presented. Slepian Basis Expansion, Linear Minimum Mean Square Error Estimation, Parallel Interference Cancellation, Minimum Mean Square Error Filtering, Soft-Input Soft-Output Decoding are the techniques implemented at the receiver. Numerical simulations with use of convolutional codes presented excellent performance in terms of Bit Error Rate vs Signal-to-Noise Ratio. Results showed how few iterations are needed to approach the Single-User Bound performance with vanishing degradation. Future works concern the extension to include use of turbo-codes for channel coding, and validation on real channels.

References

[1] J. Akhtman, L. Hanzo, "Iterative Receiver Architectures for MIMO-OFDM," *IEEE WCNC*, pp. 825–829, Mar. 2007.

[2] S.L. Ariyavisitakul, "Turbo Space-Time Processing to Improve Wireless Channel Capacity," *IEEE Trans. Commun.*, vol. 48(8), pp. 1347-1359, Aug. 2000.

[3] L.R. Bahl, J. Cocke, F. Jelinek, J. Raviv, "Optimal Decoding of Linear Codes for Minimizing Symbol Error Rate," *IEEE Trans. Inf. Theory*, vol. 20(2), pp. 284-287, Mar. 1974.

[4] S. Benedetto, D. Divsalar, G. Montorsi, F. Pollara, "A Soft-Input Soft-Output APP Module for Iterative Decoding of Concatenated Codes," *IEEE Commun. Lett.*, vol. 1(1), pp. 22-24, Jan. 1997.

[5] C. Berrou, A. Glavieux, P. Thitimajshima, "Near Shannon Limit Error-Correcting Coding and Decoding: Turbo-Codes," *IEEE ICC*, vol. 2, pp. 1064-1070, May 1993.

[6] J. Boutros, G. Caire, "Iterative Multiuser Joint Decoding: Unified Framework and Asymptotic Analysis," *IEEE Trans. Inf. Theory*, vol. 48(7), pp. 1772-1793, Jul. 2002.

[7] G. Caire, R.R. Müller, T. Tanaka, "Iterative Multiuser Joint Decoding: Optimal Power Allocation and Low-Complexity Implementation," *IEEE Trans. Inf. Theory*, vol. 50(9), pp. 1950-1973, Sep. 2004.

[8] A. Goldsmith, *Wireless Communications*, Cambridge Univ. Press, 2005.

[9] T.S. John, A. Nallanathan, M.A. Armand, "A Pilot-Aided Non-Resampling Sequential Monte Carlo Detector for Coded MIMO-Systems," *IEEE GLOBECOM*, vol. 4, pp. 2250-2254, Nov./Dec. 2005.

[10] Y. Li, J.H. Winters, N.R. Sollenberger, "MIMO-OFDM for Wireless Communications: Signal Detection with Enhanced Channel Estimation," *IEEE Trans. Commun.*, vol. 50(9), pp. 1471-1477, Sep. 2002.

[11] D.N. Liu, M.P. Fits, "Low Complexity Affine MMSE Detector for Iterative Detection-Decoding MIMO OFDM Systems," *IEEE ICC*, vol. 10, pp. 4654-4659, Jun. 2006.

[12] M. Lončar, R.R. Müller, J. Wehinger, C.F. Mecklenbräuer, T. Abe, "Iterative Channel Estimation and Data Detection in Frequency-Selective Fading MIMO Channels," *Eur. Trans. Telecommun.*, vol. 15(5), pp. 459-470, Sep./Oct. 2004.

[13] B. Lu, G. Yue, X. Wang, "Performance Analysis and Design Optimization of LPDC-Coded MIMO OFDM Systems," *IEEE Trans. Signal Process.*, vol. 52(2), pp. 348-361, Feb. 2004.

[14] R.H. Morelos-Zaragoza, *The Art of Error Correcting Coding*, John Wiley & Sons, 2002.

[15] J.G. Proakis, *Digital Communications*, McGraw Hill, 2000.

[16] T.F. Rappaport, *Wireless Communications: Principles and Practice*, 2nd Edn., Prentice Hall, 2002.

[17] P. Robertson, E. Villebrun, E. Höher, "A Comparison of Optimal and Sub-Optimal MAP Decoding Algorithms Operating in the Log Domain," *IEEE ICC*, vol. 2, pp. 1009-1013, Jun. 1995.

[18] P. Salvo Rossi, P. Pakniat, R.R. Müller, O. Edfors, "Iterative Joint Channel Estimation and Multiuser Detection for Wireless MIMO-OFDM Systems: Performance in a Real Indoor Scenario," *IEEE ISWCS*, Oct. 2007, accepted for publication.

[19] M. Sellathurai, S. Haykin, "TURBO-BLAST for Wireless Communications: Theory and Experiments," *IEEE Trans. Signal Process.*, vol. 50(10), pp. 2538-2546, Oct. 2002.

[20] D. Slepian, "Prolate Spheroidal Wave Functions, Fourier Analysis, and Uncertainty - V: The Discrete Case," *Bell Syst. Tech. J.*, vol. 57(5), pp. 13711430, May/Jun. 1978.

[21] G.L. Stüber, J.R. Barry, S.W. McLaughlin, Y. Li, M.A. Ingram, T.G. Pratt, "Broadband MIMO-OFDM for Wireless Communications," *Proc. IEEE*, vol. 92(2), pp. 271-294, Feb. 2004.

[22] D. Tse, P. Viswanath, *Fundamentals of Wireless Communications*, Cambridge Univ. Press, 2005.

[23] S. Verdú, *Multiuser Detection*, Cambridge Univ. Press, 1998.

[24] X. Wang, H.V. Poor, "Iterative (Turbo) Soft Interference Cancellation and Decoding for Coded CDMA," *IEEE Trans. Commun.*, vol. 47(7), pp. 1046-1061, Jul. 1999.

[25] T. Zemen, C.F. Mecklenbräuker, "Time-Variant Channel Estimation Using Discrete Prolate Spheroidal Sequences," *IEEE Trans. Signal Process.*, vol. 53(9), pp. 3597-3607, Sep. 2005.

[26] T. Zemen, C.F. Mecklenbräuker, J. Wehinger, R.R. Müller, "Iterative Joint Time-Variant Channel Estimation and Multi-User Detection for MC-CDMA," *IEEE Trans. Wireless Commun.*, vol. 5(6), pp. 1469-1478, Jun. 2006.

[27] Y.R. Zheng, C. Xiao, "Simulation Models with Correct Statistical Properties for Rayleigh Fading Channels," *IEEE Trans. Commun.*, vol. 51(6), pp. 920-928, Jun. 2003.